

11-25-2003

Extension and Partitioning in an Oblique Subduction Zone, New Zealand: Constraints from Three-Dimensional Numerical Modeling

Phaedra Upton

Peter O. Koons

University of Maine - Main, peter.koons@maine.edu

Donna Eberhart-Phillips

Follow this and additional works at: https://digitalcommons.library.umaine.edu/ers_facpub

 Part of the [Earth Sciences Commons](#)

Repository Citation

Upton, Phaedra; Koons, Peter O.; and Eberhart-Phillips, Donna, "Extension and Partitioning in an Oblique Subduction Zone, New Zealand: Constraints from Three-Dimensional Numerical Modeling" (2003). *Earth Science Faculty Scholarship*. 35.
https://digitalcommons.library.umaine.edu/ers_facpub/35

This Article is brought to you for free and open access by DigitalCommons@UMaine. It has been accepted for inclusion in Earth Science Faculty Scholarship by an authorized administrator of DigitalCommons@UMaine. For more information, please contact um.library.technical.services@maine.edu.

Extension and partitioning in an oblique subduction zone, New Zealand: Constraints from three-dimensional numerical modeling

Phædra Upton¹ and Peter O. Koons¹

Geology Department, University of Otago, Dunedin, New Zealand

Donna Eberhart-Phillips

Institute of Geological and Nuclear Sciences, Dunedin, New Zealand

Received 26 June 2002; revised 15 August 2003; accepted 15 October 2003; published 25 November 2003.

[1] Contraction, strike slip, and extension displacements along the Hikurangi margin northeast of the North Island of New Zealand coincide with large lateral gradients in material properties. We use a finite-difference code utilizing elastic and elastic-plastic rheologies to build large-scale, three-dimensional numerical models which investigate the influence of material properties on velocity partitioning within oblique subduction zones. Rheological variation in the oblique models is constrained by seismic velocity and attenuation information available for the Hikurangi margin. We compare the effect of weakly versus strongly coupled subduction interfaces on the development of extension and the partitioning of velocity components for orthogonal and oblique convergence and include the effect of ponded sediments beneath the Raukumara Peninsula. Extension and velocity partitioning occur if the subduction interface is weak, but neither develops if the subduction interface is strong. The simple mechanical model incorporating rheological variation based on seismic observations produces kinematics that closely match those published from the Hikurangi margin. These include extension within the Taupo Volcanic Zone, uplift over ponded sediments, and dextral contraction to the south.

INDEX TERMS: 8020 Structural Geology: Mechanics; 8159 Tectonophysics: Rheology—crust and lithosphere; 3210 Mathematical Geophysics: Modeling; 8109 Tectonophysics: Continental tectonics—extensional (0905); 1206 Geodesy and Gravity: Crustal movements—interplate (8155); **KEYWORDS:** numerical modeling, Hikurangi trench, subduction interface strength, plate coupling, partitioning. **Citation:** Upton, P., P. O. Koons, and D. Eberhart-Phillips, Extension and partitioning in an oblique subduction zone, New Zealand: Constraints from

three-dimensional numerical modeling, *Tectonics*, 22(6), 1068, doi:10.1029/2002TC001431, 2003.

1. Introduction

[2] Strain characteristics within the upper plates of subduction systems can vary greatly between and within subduction zones [e.g., *Uyeda and Kanamori*, 1979; *Dewey*, 1980; *Uyeda*, 1982]. This study addresses the subduction-related processes of extension and partitioning of velocity components in an oblique subduction zone, using the Hikurangi margin of New Zealand as an example. Using large-scale, three-dimensional, finite-difference numerical modeling we show that strain within an oblique subduction zone is influenced by intraplate strength.

[3] Extensional systems are associated with many subduction zones worldwide, and there are a number of theories which attempt to explain the mechanics behind their existence [e.g., *Molnar and Atwater*, 1978; *Uyeda and Kanamori*, 1979; *Dewey*, 1980; *Uyeda*, 1982; *Whittaker et al.*, 1992; *Hamilton*, 1995; *Hassani et al.*, 1997]. Although slab rollback is commonly cited as the accepted mechanism for extension above subduction zones [*Molnar and Atwater*, 1978; *Hamilton*, 1995], neither this nor other current models adequately specify necessary and/or sufficient conditions for extensional tectonics in a convergent setting [*Taylor and Karner*, 1983; *Scholz and Campos*, 1995]. Models in two dimensions of the forces associated with subduction suggest that an unlocked subduction interface is required to develop appreciable tension in a back arc setting [*Whittaker et al.*, 1992; *Hassani et al.*, 1997].

[4] Some oblique subduction zones exhibit strain partitioning, where two processes accommodate the oblique plate motion: subduction with lesser obliquity and trans-current faulting within the overriding plate. Different authors have proposed various explanations for this phenomenon [e.g., *Jarrard*, 1986; *McCaffrey*, 1992; *Liu et al.*, 1995]. Many authors cite interplate coupling as a basic factor controlling the partitioning, although they do not agree on the details. Some authors suggest that partitioning occurs when plate coupling is strong [*Finch*, 1972; *Beck*, 1983; *Jarrard*, 1986; *Chemenda et al.*, 2000], while others reach the opposite conclusion [*Yu et al.*, 1993; *Liu et al.*,

¹Now at Department of Earth Sciences, University of Maine, Orono, Maine, USA.

1995]. An alternative explanation for partitioning is that oblique slip parallel to the plate vector should occur on the thrust fault when the obliquity is smaller than a critical angle [McCaffrey, 1992]. If this were the case, partitioning would be expected to occur for high angles of obliquity but not for small.

[5] Different definitions of coupling are used in the analysis of subduction plate boundaries, and the following terminology, based on that of Beanland's [1995] analysis of the Hikurangi Trough, is used to distinguish between them.

[6] 1. Seismic coupling is the rate of actual seismic moment release as a proportion of the total seismic moment release expected due to relative motion across a plate boundary [Ruff, 1989; Pacheco et al., 1993].

[7] 2. Kinematic coupling describes the rate of permanent deformation, seismic or not, accommodated in the upper plate as a proportion of relative plate motion across a plate boundary [McCaffrey, 1992; Beanland, 1995].

[8] 3. Dynamic coupling is defined in terms of forces and stresses, with the most important factor being the frictional strength of the subduction interface at shallow depths [Scholz and Campos, 1995]. One extreme of dynamic coupling is that the interface may be stronger than the upper plate, resulting in a high degree of kinematic coupling. Alternatively, if the subduction interface is significantly weaker, stable sliding will occur and the interface is considered to be dynamically uncoupled [Scholz and Campos, 1995].

[9] In this study we are describing coupling of the two components of displacement, which is equivalent to kinematic coupling.

[10] We use northern New Zealand and the Hikurangi Trough as a basis for three-dimensional (3-D) numerical models that investigate various features of subduction zones and their effect on the resulting geodynamics. The Hikurangi subduction zone, which shows considerable variance in strain characteristics, coupling and partitioning along its 500 km length, provides an ideal comparison for our models. We argue in this paper that the strength of the subduction interface is the dominant factor determining the amount of displacement coupling and therefore controls the nature of velocity component partitioning between the subduction interface and the upper plate. Moreover, we infer that a weak subduction interface is required for both extension and partitioning to occur in a subduction zone with geometry similar to that of the Hikurangi margin.

2. Hikurangi Subduction Margin

[11] Subduction of the Pacific plate beneath the Australian plate at the southernmost end of the Tonga-Kermadec-Hikurangi plate boundary is the dominant tectonic feature of the North Island and the northern South Island (Figure 1). Deformation on-land in the North Island falls into two main provinces: a belt of dextral faulting generally near the back edge of the inner forearc region; and normal faulting in the Ruamoko Rift System (Figure 1) [Grindley, 1960; Rowland and Sibson, 2001]. Offshore, landwards of the

trench, is a zone of imbricate reverse faulting [Barnes et al., 1998; Beanland et al., 1998].

2.1. Kinematic Coupling Along the Hikurangi Margin

[12] A detailed analysis of partitioning of margin-parallel and margin-normal displacement along the Hikurangi subduction margin was carried out by Beanland [1995]. The range of mechanical and kinematic behavior observed along the Hikurangi margin is consistent with a transition in dynamic coupling from totally coupled in the south to uncoupled with arc/back arc extension in the north. Beanland [1995] points out that this wide range of behavior over a length scale of only 500 km occurs despite uniformity in geometry, absolute rates of motion and plate motion obliquity along the Hikurangi margin [DeMets et al., 1994]. Beanland suggested that the range in dynamic coupling arises primarily as a result of the depth extent of the subducted Pacific plate which decreases to the south.

2.2. Morphology of the Hikurangi Subduction Zone

[13] The general shape of the subducted Pacific plate at the Hikurangi margin has been imaged by compilations of seismicity located within the New Zealand National Seismograph Network [Anderson and Webb, 1994]. The seismic zone associated with the subducted plate dips to the NW, $\sim 11^\circ$, steepening with depth, and has a strike of 40° [Ansell and Bannister, 1996]. A model of plate coupling along the Hikurangi subduction zone has been developed from seismological data [Reyners, 1998]. There is a major change from permanent coupling in Marlborough, over the last ~ 4 Ma, to weak coupling in the northeast of the Raukumara Peninsula [Reyners, 1998]. The shortening within the overlying plate perpendicular to the margin in the southern North Island and northern South Island arises from the locking of the plate interface in this region [Whittaker et al., 1992; Reyners, 1998]. Changes in coupling along strike imply sinistral shear in the subducting plate and/or dextral shear in the overlying plate [Reyners, 1998].

[14] The NW portion of Raukumara Peninsula is experiencing broad antiformal uplift (3 mm yr^{-1} over the past 125 kyr) along the Raukumara Range [Yoshikawa et al., 1980; Thornley, 1996]. Rapid uplift of the Raukumara Range has been interpreted by Walcott [1987] as being due to sediment subduction and underplating at the base of the crust of the Australian plate. The subducted slab, the plate interface and variations in the overlying plate structure of the Raukumara Peninsula have been imaged in a 3-D seismic velocity and attenuation model [Reyners et al., 1999; Eberhart-Phillips and Chadwick, 2002]. Waveform modeling indicates a 1–2 km thick low-velocity layer at the plate interface, which is characterized by $\sim 50\%$ local reduction in shear modulus and inferred to consist of subducted sediments [Eberhart-Phillips and Reyners, 1999]. Mechanically this ponded sediment may result in relatively weak plate coupling in this region [Eberhart-Phillips and Reyners, 1999]. Seismic velocity determinations also show an extensive low-velocity zone in the lower crust, interpreted by the authors to be a region of ponded sediment beneath the northeastern Raukumara Range [Reyners et al., 1999, Figure 8]. We use

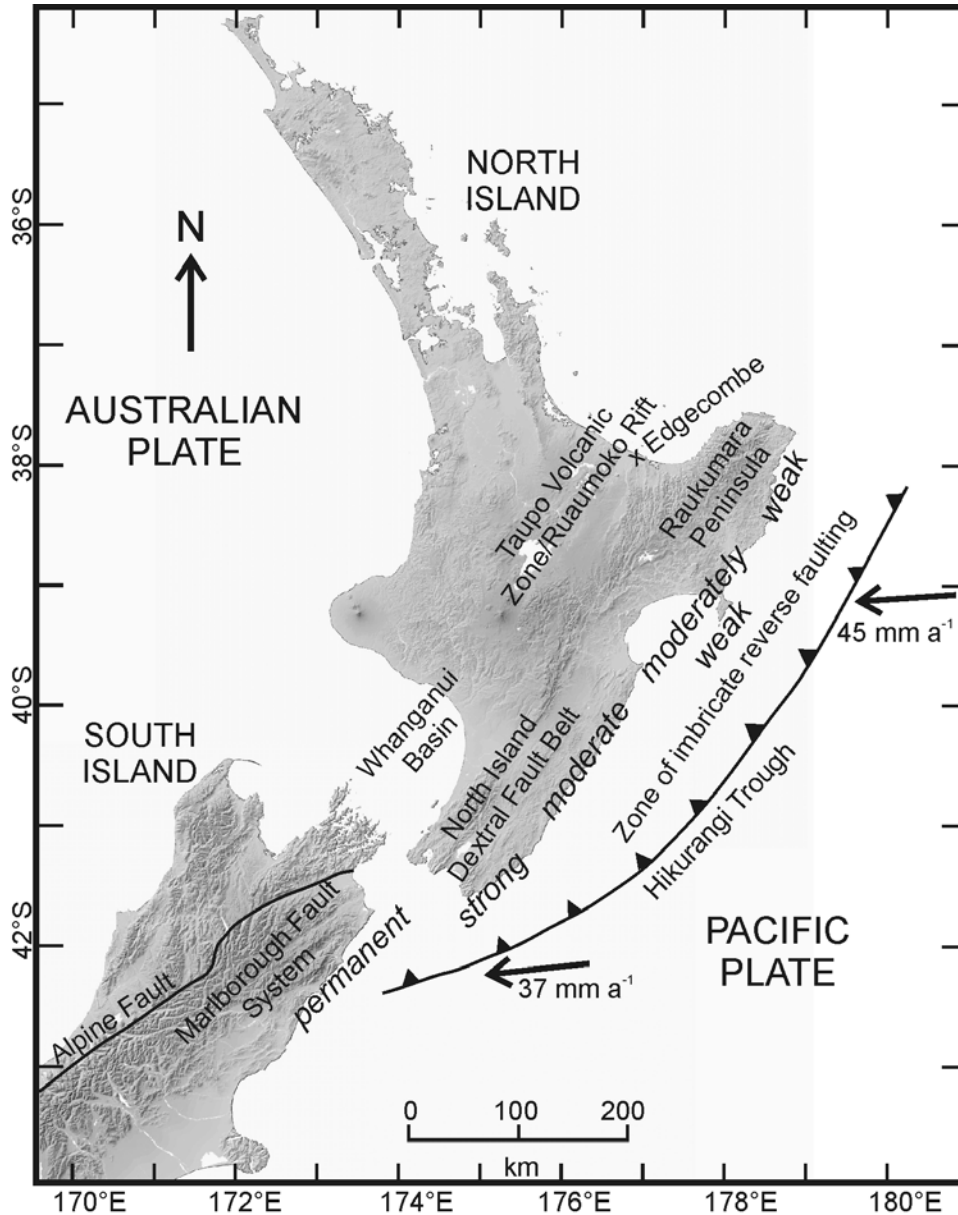


Figure 1. Northern New Zealand showing the Hikurangi Trough and associated deformation zones in the Australian plate, the Marlborough fault system and the Alpine fault. The interpreted degree of plate coupling along the Hikurangi subduction margin is shown in italics [Reyners, 1998]. Relative plate motion vectors between the Australian and Pacific plates are from DeMets *et al.* [1994]. Shaded relief map from GeographX.

seismic velocities determined for this region [Reyners *et al.*, 1999] to calculate elastic and inelastic material properties for input into a model of this area. This low-velocity zone underlies the most rapidly rising part of the Raukumara Ranges and may be related to that uplift [Reyners *et al.*, 1999]. We test the hypothesis that the presence of these low-velocity sediments is responsible for the surface uplift.

2.3. Deformation Within Northern New Zealand

[15] Quaternary continental extension within the central North Island is accommodated by a belt of predominantly

normal faults, known as the Ruaumoko Rift (Figure 1) [Grindley, 1960]. It is a zone of NE striking active normal faults, dikes and extension-fracturing extending the length of the Taupo Volcanic Zone and distributed across a region ~40 km wide [Rowland and Sibson, 2001]. The focal mechanism solution from the 1987 Edgecumbe earthquake shows that it was a mainly normal rupture with a small component of dextral strike-slip motion [Anderson *et al.*, 1990].

[16] The forearc region in the south of the North Island is dominated by north to northeast striking reverse faults

[Beanland *et al.*, 1998]. These faults are parallel to the subduction margin and show dextral reverse motion. The total shortening accommodated along them is on the order of $\geq 50\%$ of plate motion [Beanland *et al.*, 1998].

[17] Focal mechanisms from interplate thrust earthquakes along the Hikurangi margin indicate that seismically released oblique plate motion across the margin is fully partitioned along the whole length of the margin [Webb and Anderson, 1998]. Shortening occurs along the plate interface while it accommodates very little of the transcurrent motions [Webb and Anderson, 1998]. Instead, faults in the overlying Australian plate accommodate most of the transcurrent motion in the southwest [Webb and Anderson, 1998], and it is proposed that rotation due opening of the Taupo Volcanic Zone accommodates this motion in the northeast [Beanland and Haines, 1998]. Geodetic measurements across the plate boundary zone show extension in the crust in the northeast and shortening across the margin in the southwest [Walcott, 1984; Beanland and Haines, 1998]. The geodetic measurements in the southwest do not show the partitioning seen in focal mechanism studies [Webb and Anderson, 1998]. Barnes *et al.* [1998] propose a complex pattern of partitioning of strain both vertically and horizontally between the two plates and within the upper plate for the southwest Hikurangi margin. They determine that subduction accounts for $< 20\%$ of margin-parallel motion and that one third to one half of total plate motion is expressed in the upper plate offshore. These results are consistent with analysis onshore and reflect the strong coupling between the subducted plate and the overriding Australian plate [Beanland, 1995].

3. Theoretical Background

3.1. Mechanical Relationships

[18] The mechanical behaviors of the materials modeled here are elastic or nonassociated elastic-plastic [Vermeer and de Borst, 1984]. For the constitutive rules, we use both Mohr-Coulomb and Von Mises criteria. These consist of a yield function, which governs the onset of plastic behavior, and a plastic flow rule. These materials deform in an elastic manner up to a yield point, then deform in a plastic (i.e., nonrecoverable) manner. For a Mohr-Coulomb material the yield function and flow law are given as

$$f = \tau + \sigma \sin \phi - C \cos \phi$$

$$g = \tau + \sigma \sin \psi + \text{constant}$$

The Von Mises criteria is given by

$$f = \tau - k_\phi$$

$$g = \tau - \psi \sigma$$

where

f	yield function
g	flow law
τ	maximum shear stress (Pa)
σ	mean stress (Pa)

ϕ	internal friction angle ($^\circ$)
C	cohesion (Pa)
ψ	dilation angle ($^\circ$)
k_ϕ	shear strength (Pa)
q_ψ	post failure component (Pa).

[19] The Mohr-Coulomb flow stress during plastic deformation is strongly pressure-dependent and is useful for modeling the upper, brittle crust. The Von Mises flow strength is used to model the ductile lower crust. In the plastic regime, instability or localization occurs, which for rock corresponds to a well-defined shear zone or a fracture [Vermeer and de Borst, 1984; Mandl, 1988; Hobbs *et al.*, 1990; Ord and Oliver, 1997].

3.2. Finite-Difference Code

[20] Models were developed using the numerical code FLAC^{3D} a three-dimensional finite-difference code, which we have modified to accommodate large strains and local erosion (Version 2.0, Fast Lagrangian Analysis of Continua in Three Dimensions [Cundall and Board, 1988]). A large number of comparisons have been made between FLAC^{3D} results and exact solutions for plasticity problems [ITASCA, 1997]. The results show uniformly good agreement with theoretical solutions and in modeling geometrical instabilities well past the collapse or failure limit. Materials are represented by polyhedral elements within a three-dimensional grid that uses an explicit, time-marching solution scheme and a form of dynamic relaxation. Each element behaves according to a prescribed linear or nonlinear stress/strain law in response to applied forces or boundary restraints. The inertial terms in the equations of motion,

$$\frac{\partial \sigma_{ij}}{\partial x_i} + \rho b_i = \rho \frac{dv_i}{dt}$$

(Cauchy's equations of motion where σ_{ij} is the stress tensor, x_i , v_i are the vector components of position and velocity respectively ρ is the density of the material, b_i is the body force) are used as a numerical means to reach the equilibrium state of the system under consideration. The resulting system of ordinary differential equations is then solved numerically using an explicit finite-difference approach in time. The drawbacks of the explicit formulation (i.e., small time step limitation and the question of required damping) are overcome by automatic inertia scaling and automatic damping that does not influence the mode of failure. The governing differential equations are solved alternately, with the output for the solutions of the equations of motion used as input to the constitutive equations for a progressive calculation. Solution is achieved by approximating first-order space and time derivatives of a variable using finite differences, assuming linear variations of the variable over finite space and time intervals, respectively. The continuous medium is replaced by a discrete equivalent with all forces involved concentrated at the nodes of a three-dimensional mesh used in the medium representation.

3.3. Models

[21] We use an elastic slab that subducts beneath a two-layer upper plate (Figure 2). The upper brittle crust is given

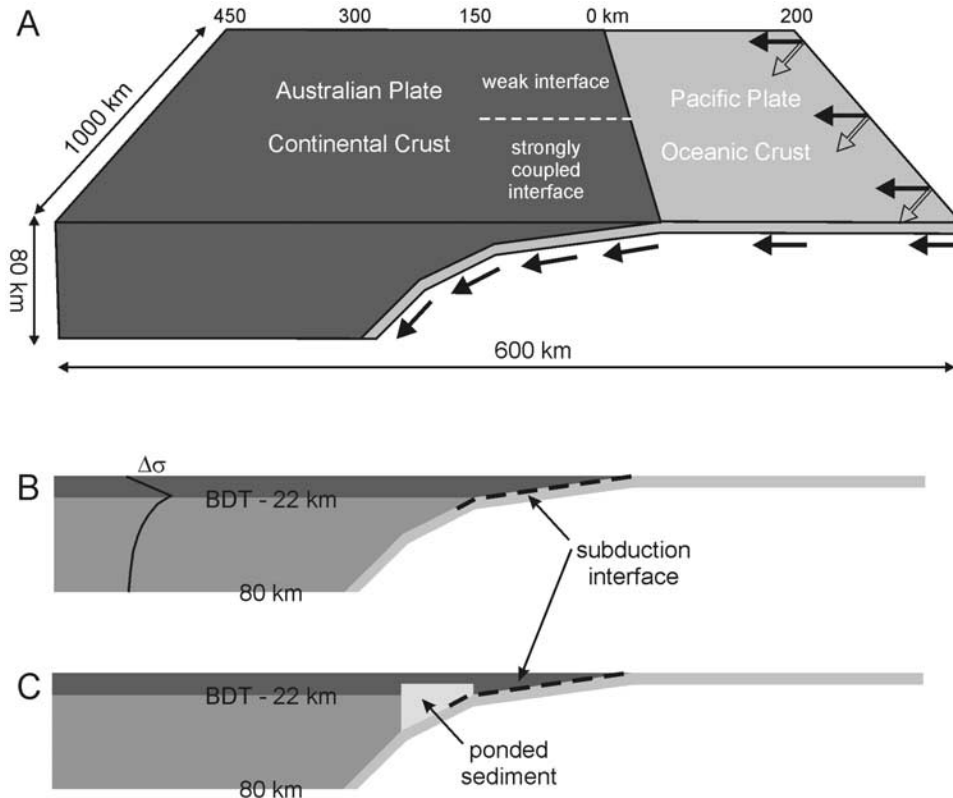


Figure 2. (a) Block diagram of the geometry used in the models. The boundary conditions are put on to the oceanic slab as velocity vectors. Two sets of velocity boundary conditions are shown; filled arrows show orthogonal subduction while open arrows are those for oblique subduction with $v_x:v_y$ equal to 1:1. The strength of the subduction interface is varied from weak in the north to strong in the south. (b and c) Cross sections showing material properties for different regions of the models. Figure 2b is the standard model in which the strength of the subduction interface is varied. Strength profile ($\Delta\sigma$ = differential strength) shows how the strength of the model varies with depth. Figure 2c is the model of the Raukumara Peninsula where a block of weaker material represents ponded sediment as discussed in the text [Eberhart-Phillips and Reyners, 1999; Reyners et al., 1999]. BDT, brittle-ductile transition.

an elastic-plastic rheology based on a Mohr-Coulomb yield condition and flow law. The material beneath the brittle-ductile transition is given an elastic-plastic rheology based on a Von Mises yield condition and flow law. This material gets weaker with depth, mimicking the temperature dependence of lithospheric strength (Figure 2b). The subduction interface is modeled using a pressure-dependent Mohr-Coulomb constitutive relationship to a depth of 22 km, corresponding to the average depth of the seismic coupling beneath the North Island [Reyners, 1998].

[22] The model material is a continuum, with no discrete discontinuities, thus the seismic cycle is not explicitly modeled. We are using the models to investigate long-term strain patterns within the upper plate of a subduction system. This approach is best suited to investigation of the two extremes of plate interface strength. These are a weak interface, where deformation is taken up mainly along the interface, and a strong interface where deformation is taken up within the upper plate. Aspects of moderate or strong plate interfaces along which deformation occurs by large seismic events are not well modeled by a continuum

approach and care must be taken not to overinterpret models of these types of subduction interface.

[23] We have run a series of models in which we change the strength of the subduction interface along strike (Figure 2). We simplify Reyners' [1998] description of varying interface strength along the margin into two regions, weak in the northeast and strong in the southwest (Figure 2). Our other models investigate the effects of variations in the strength of regions within the overlying plate. The details of these are discussed below.

[24] The model is 1000 km along strike and 600 km across the plate boundary zone, from undeformed oceanic crust of the Pacific plate in the east to undeformed continental crust of the Australian plate in the west (Figure 2). The base of the model is at 80 km depth, with the brittle-ductile transition located at the depth of 22 km. The oceanic crust of the Pacific plate is modeled by an 8 km thick elastic slab. The subduction interface is modeled by a 1 km thick series of zones that sit above the elastic material of the oceanic plate. These zones are not constrained in any way by the imposed boundary conditions. From 0–22 km, the

subduction interface is modeled as a pressure-dependent Mohr-Coulomb material. Below 22 km, it is described by a Von Mises flow law. Variations in strength of the subduction interface are imposed on the upper 22 km by changing the value of the friction angle within the Mohr-Coulomb description.

[25] Velocity conditions are imposed upon the base, the eastern and the lateral edges of the elastic material that represents the subducting Pacific plate (Figure 2). The orientation of the imposed velocity conditions is varied from orthogonal to the plate boundary to 60° oblique to the plate boundary. Imposed velocity conditions where subduction is occurring at 45° to the trench most closely match the Nuvel-1a Pacific plate motion relative to fixed Australia plate [DeMets *et al.*, 1994]. We therefore concentrate on two models, one orthogonal model with subduction perpendicular to the trench and one oblique model with subduction occurring at 45° to the trench. The western boundary, within undeformed Australian plate material, is held fixed. The basal boundary, at 80 km depth, is also held fixed. The aim of this study is to investigate processes within the upper plate of the subduction system, and the boundary at 80 km depth is far enough removed from the region of interest so as not to impinge upon the results. The models ignore the influence of deeper processes and features such as the density contrast of the lithospheric slab and the asthenosphere.

4. Results

4.1. Orthogonal Subduction; Variable Interfacial Strength

[26] In order to consider the effect of the strength of the plate interface on the mechanics of subduction, we initially consider orthogonal subduction of the Pacific plate beneath the Australian plate (Figure 3). In these models, the subduction interface is weaker to the north than the overlying plate while in the south the interface is stronger than the overlying plate. With a weak subduction interface, deformation at the surface takes place at the trench and within the upper plate at ~200–300 km west of the trench, above the ductile portion of the subduction interface (Figure 3a). Localized deformation at the subduction interface takes place from the trench to a depth of ~40 km (Figure 3b). At greater depths the deformation is more diffuse. A region of extension develops within the upper plate well away from the trench. Total extension is ~5% of the imposed velocity boundary condition.

[27] Where the subduction interface is strong, deformation within the upper plate and localized deformation of the interface both occur away from the trench, at ~150–300 km from the trench, above where the two plates are no longer strongly coupled. There is no region of extension behind a strong subduction interface. These results are similar to those produced by two-dimensional models without along-strike heterogeneities [Whittaker *et al.*, 1992; Hassani *et al.*, 1997].

[28] Above the sharp transition from a strong interface to a weak interface there is a large gradient in the margin-

normal velocity (Figure 3a) corresponding to dextral movement perpendicular to the trench. In other models with a smaller variation in strength, less pronounced zones of dextral displacement are produced.

[29] The downward motion of the model slab produces negative vertical velocities and the formation of an elongate basin structure in the upper plate (Figure 3c). This basin forms along the whole model and is not a result of the region of extension. Where the subduction interface is weak, the zone with negative velocities is narrow and nearly symmetric. With a strong subduction interface, the zone of material with negative velocities is wider and the deepest part of the basin is offset toward to the trench, above the transition from a strongly coupled interface to that of to a ductile subduction.

4.2. Oblique Subduction; Variable Interfacial Strength

[30] Imposition of oblique boundary conditions leads to the potential for the development of partitioning of the two components of velocity, margin-parallel and margin-normal. Where the subduction interface is weak, the two components of deformation are partitioned (Figures 4a and 4b). The majority of the margin-normal component is taken up at the trench, along the subduction interface, with the residual taken up within the upper plate at a distance of 200–300 km from the trench. The margin-parallel component is taken up within the upper plate, ~150–300 km from the trench. In contrast, the two components of velocity do not partition above the strong plate interface (Figures 4a and 4b). In this instance, the margin-parallel and the margin-normal components of the motion are taken up together, within the upper plate, 150–300 km west of the trench. The obliquity of the boundary conditions affects the graben development in that it becomes deeper and more pronounced in the south (Figure 4c). Otherwise the pattern of vertical displacement is similar to that of the orthogonal model.

[31] Models were also run with the angle of obliquity equal to 15°, 30°, and 60°. As in the model with $v_x = v_y$ (angle of obliquity equal to 45°), partitioning occurred for a weak subduction interface but not for a strong subduction interface.

4.3. Model of the Raukumara Peninsula; Oblique Subduction; Homogeneous Interfacial Strength

[32] In this model the entire subduction interface is given a strength between the weak and strong extremes of the previous two models, less than that of the overlying Pacific plate material. A region simulating soft ponded sediment is put into the northern half of the model (Figure 2c). This has the effect of localizing most of the plate-normal and plate-parallel velocity in the region of the weaker sediment (Figures 5a and 5b). No partitioning of the two velocity components occurs except in the west where a zone of extension develops within the Australian plate. A region of uplift develops to the east of the extension and basin formation within the upper plate (Figure 5c). To the south, where the subduction interface is of average strength, the deformation is spread relatively evenly between the trench

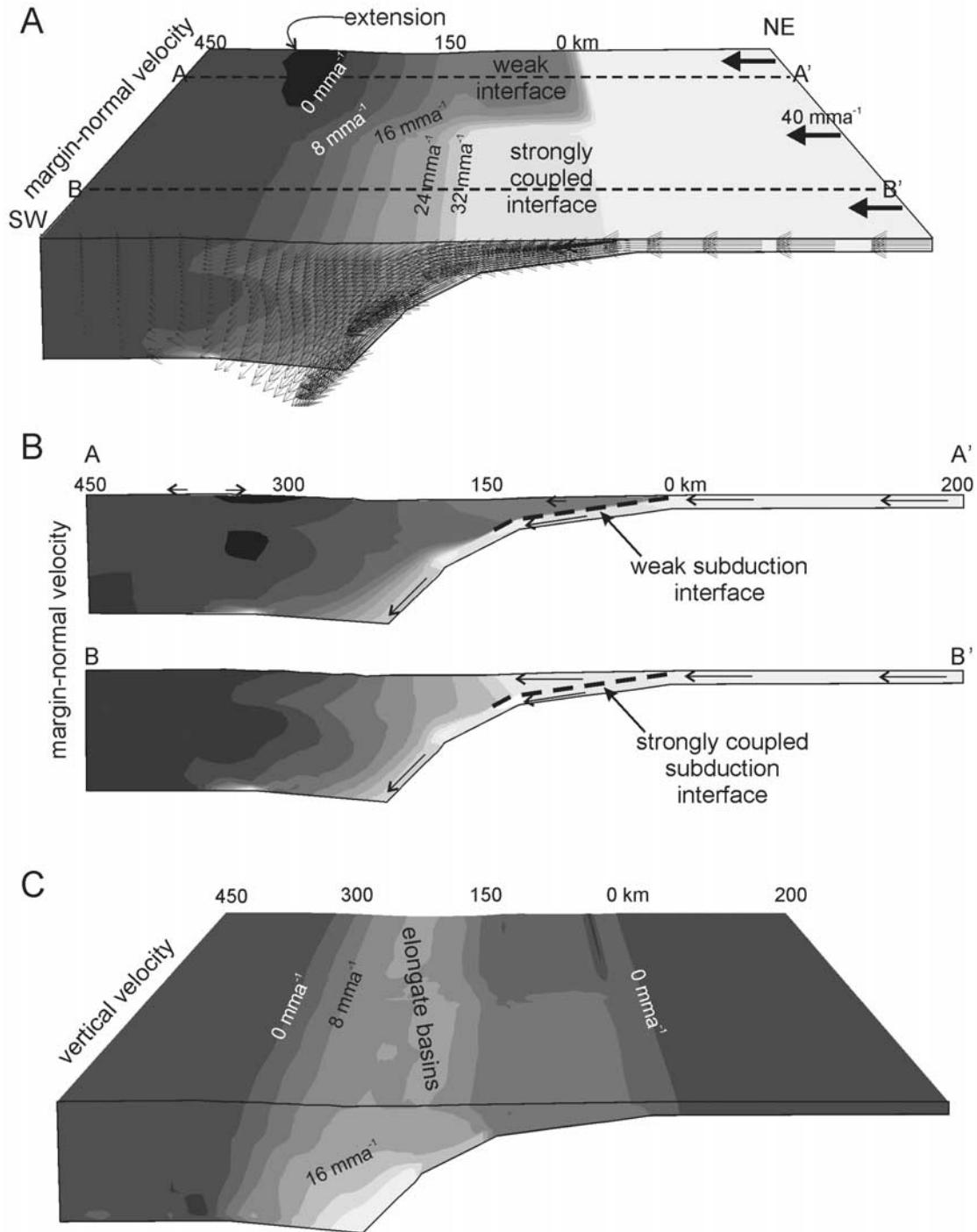


Figure 3. Model of orthogonal subduction. (a) Contours of margin-normal velocity where pale gray is the plate motion magnitude and dark gray is zero velocity. The region of black represents velocity in the opposite direction to the plate motion. (b) Cross sections (locations shown in Figure 3a) of margin-normal velocity showing the region of extension that develops in the north. Note that vectors are not to scale. (c) Contours of vertical velocity where light gray is maximum negative and dark gray is no vertical movement. For all contour plots and all velocity components, the contour interval is 4 mm yr^{-1} corresponding to the motion of the Pacific plate relative to fixed Australia equal to 40 mm yr^{-1} .

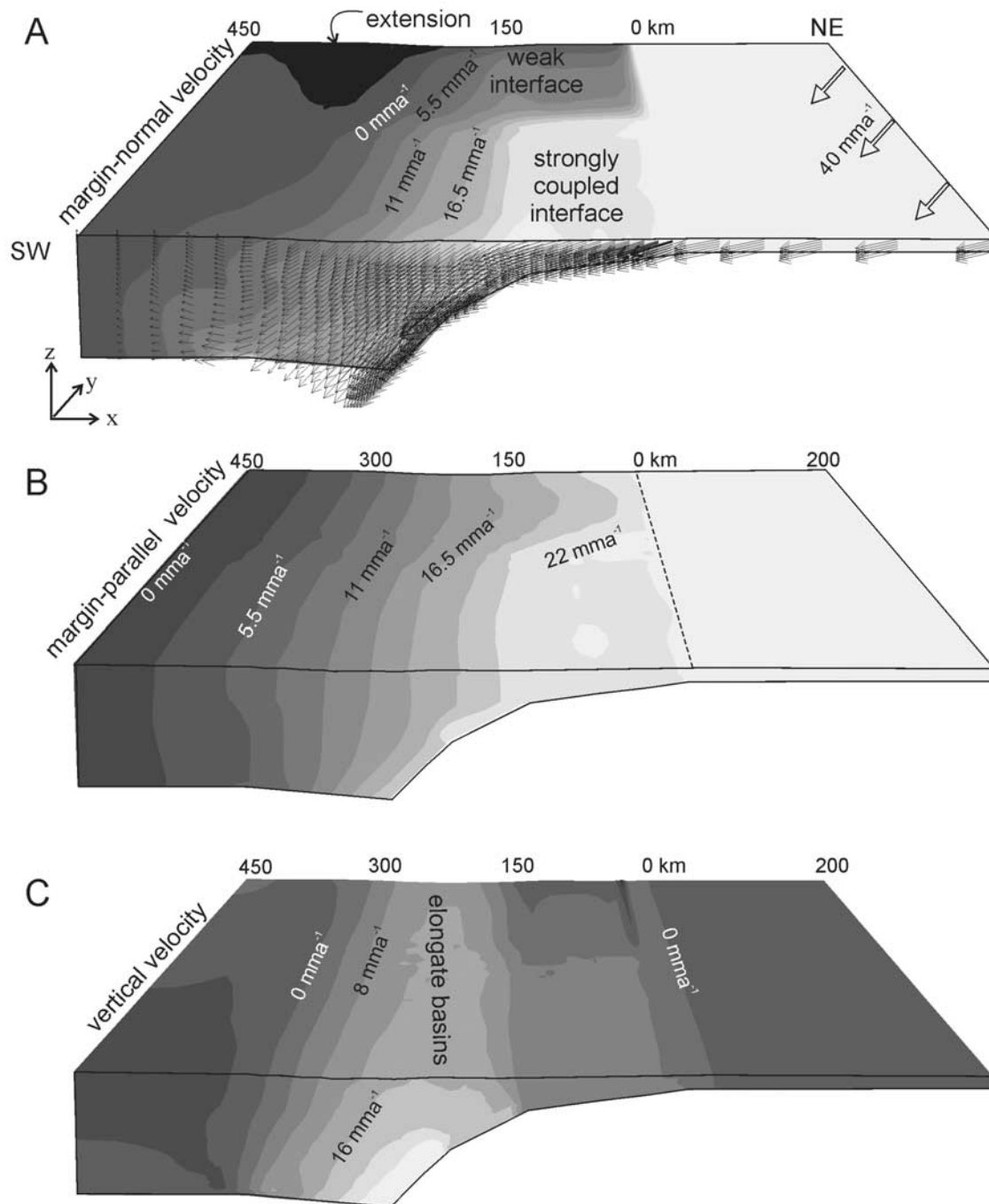


Figure 4. Model of oblique subduction. (a) Contours of margin-normal velocity where pale gray is the plate motion magnitude and dark gray is zero velocity. The region of black represents velocity in the opposite direction to the plate motion. (b) Contours of margin-parallel velocity; pale gray is the plate motion magnitude and dark gray is zero velocity. (c) Contours of vertical velocity where light gray is maximum negative and dark gray is no vertical movement. For margin-parallel and margin-normal contour plots, the contour interval is 2.75 mm yr^{-1} and for vertical velocity, the contour interval is 4 mm yr^{-1} .

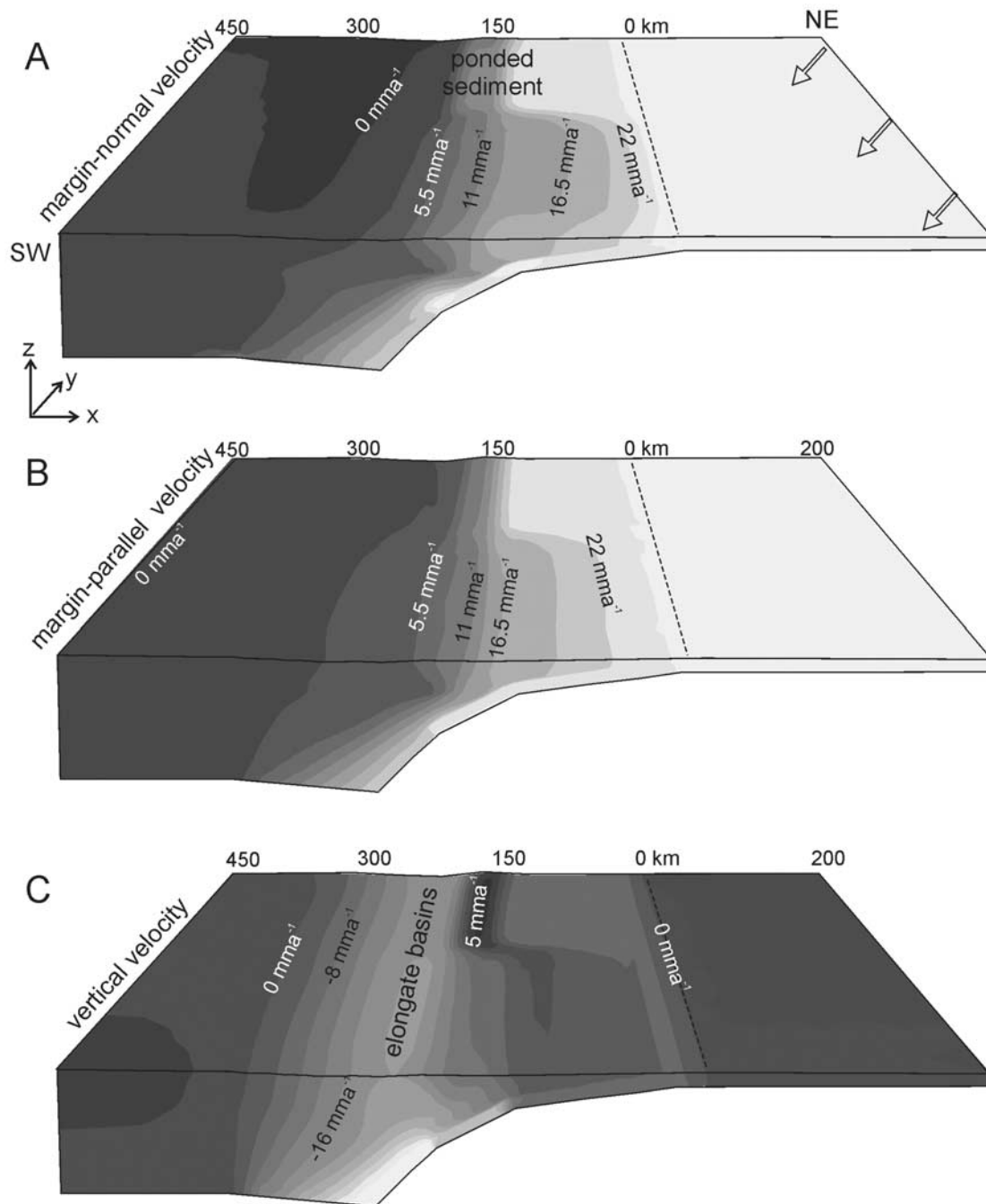


Figure 5. Model of the Raukumara Peninsula. (a) Contours of margin-normal velocity where pale gray is the plate motion magnitude and dark gray is zero velocity. The region of black represents velocity in the opposite direction to the plate motion. (b) Contours of margin-parallel velocity; pale gray is the plate motion magnitude and dark gray is zero velocity. (c) Contours of vertical velocity where light gray is maximum negative and dark gray is no vertical movement. For margin-parallel and margin-normal contour plots, the contour interval is 2.75 mm yr^{-1} and for vertical velocity, the contour interval is 4 mm yr^{-1} .

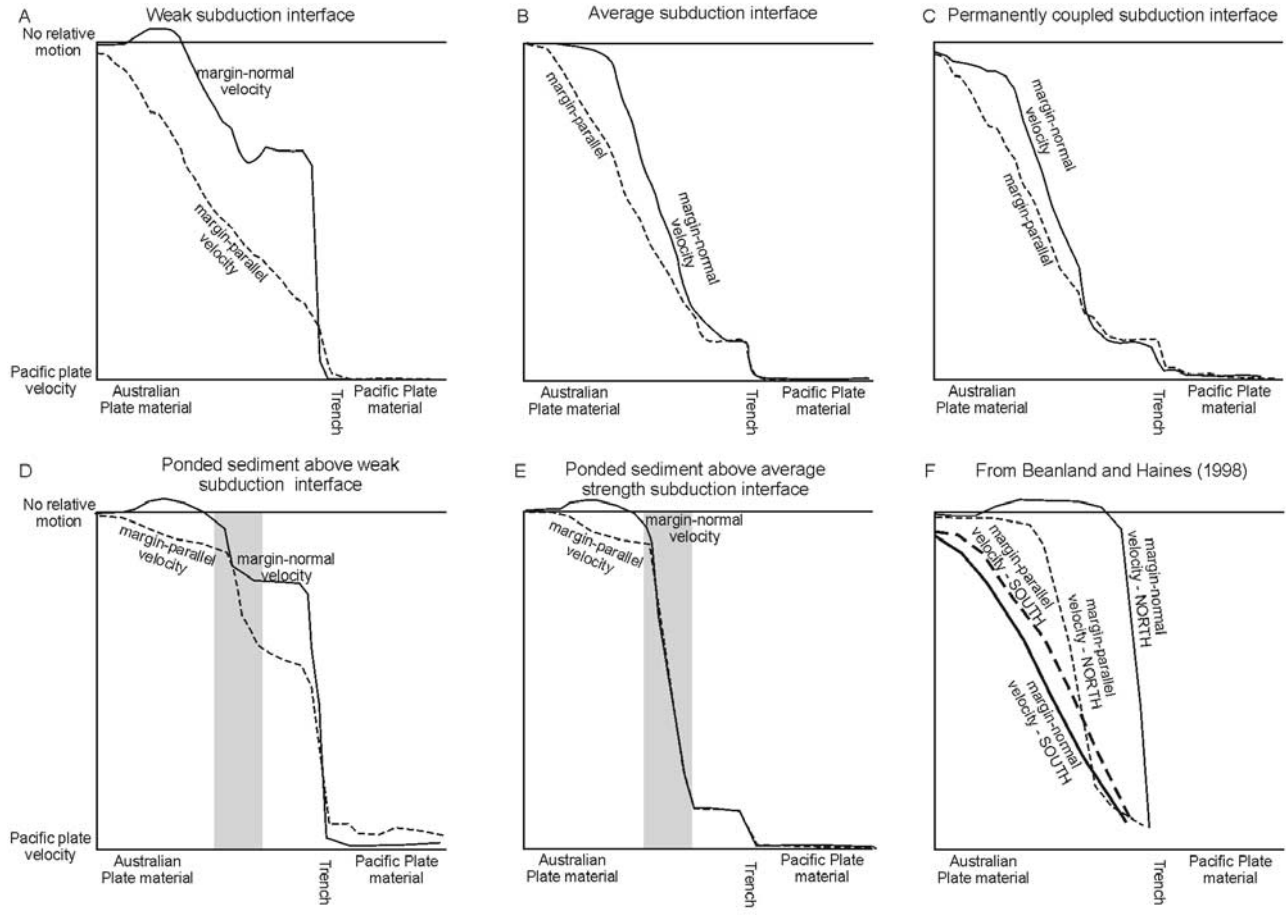


Figure 6. Plots of margin-normal velocity and margin-parallel velocity components across the northern and southern transects of the three oblique models. (a) Partitioning of velocity components above a weak subduction interface. (b) Partitioning of velocity components above an average strength subduction interface. (c) Partitioning of velocity components above a strong subduction interface. (d) Partitioning of velocity components above a weak subduction interface where the upper plate contains a region of weaker material representing ponded sediment. (e) Partitioning of velocity components above an average strength subduction interface where the upper plate contains a region of weaker material representing ponded sediment. (f) Approximate partitioning of velocity components from *Beanland and Haines* [1998]. Care must be taken when considering the offshore interpretation as the data (geological and geodetic) in this region are very limited.

and the undeformed Australian plate on the western edge of the model.

4.4. Model of the Raukumara Peninsula; Oblique Subduction; Variable Interfacial Strength

[33] This model combines the previous models to gauge the combined effect of a weak subduction interface with a region of ponded sediment above the subduction interface. In the south, the model is unchanged from the model of oblique subduction with a strong subduction interface. In the north, the region of ponded sediment sits above a weak subduction interface. The margin-normal velocity is similar to the model without the ponded sediment. There is a significant region of extension to the west of the subduction, similar to the previous model. Unlike any of the previous

models, there is a significant margin-parallel velocity gradient at the trench, such that the form of the gradient in margin-parallel velocity is similar to the form of the gradient in margin-normal velocity (Figure 6).

4.5. Partitioning of Margin-Normal and Margin-Parallel Velocity Components

[34] Figure 6 shows the variation across the subduction zone of the components of margin-normal and margin-parallel velocities for the three oblique models. From these plots we can state the conditions under which partitioning of velocity components will occur.

[35] A weak subduction interface results in partitioning of velocity components across the whole subduction zone (Figure 6a). A strong or average-strength subduction inter-

face leads to only a small degree of partitioning away from the trench (Figures 6b, 6c, 6d, and 6f). Close to the trench, the two velocity gradients are nearly identical.

[36] The presence of ponded sediment, which is weaker than the surrounding material, above the subduction interface causes the degree of partitioning, for a particular interface strength, to reduce markedly (Figures 6d and 6e). If the subduction interface is weak, the motion is partitioned west of the trench and at the western edge of the deforming region (Figure 6d). Above the ponded sediment, the gradient of margin-parallel velocity component increases such that the two components are much closer than they were for the model with a weak subduction interface. When the subduction interface is of average strength, partitioning only occurs where the change from horizontal to downward motion of the trench causes the margin-normal component of velocity to become extensional (Figure 6e).

5. Implications for Extension and Partitioning at Subduction Margins

5.1. Upper Plate Extension as a Function of Interfacial Strength

[37] Our numerical models have shown that extension will develop behind a subduction system, with geometry similar to the Hikurangi margin, if the subduction interface is significantly weaker than the material in the overlying plate. We do not develop extension behind a system with a strong subduction interface. These models provide an explanation for extension where the existence of slab rollback is unconfirmed. The results support *Whittaker et al.*'s [1992] assertion that an unlocked subduction interface is required to develop tension within the upper plate.

[38] Where the subduction interface is strong, the upper plate is forced to move with the slab. West of the trench, at about $x = 150$ km, once the subduction interface is located below the brittle-ductile transition, movement can be taken up along the interface. Upper plate deformation in this region is compressional (Figure 3b). For the weak interface, from $x = 0$ to 150 km, the slab and the upper plate are decoupled such that the slab moves along beneath the upper plate. As some of this subhorizontal westward motion is converted to downward motion with the steepening of the slab, the slab continues to move beneath the upper plate but at a reduced horizontal rate. This reduction in the amount of horizontal motion of the slab beneath the upper plate results in space generation within the upper plate and this is manifest as a region of extension (Figure 3b).

[39] The amount of extension that develops in these models is on the order of 5% of the imposed plate boundary (Figure 6a). This value is a function of the slab angle and would increase if the slab dipped more steeply and would go to zero for a shallowly dipping slab.

5.2. Partitioning as a Function of Interfacial Strength

[40] Using the geodynamic models described above, we can make a number of predictions about partitioning of

velocity components at a subduction margin, based on the relative strengths of the subduction interface and the upper plate material (Figure 6). Firstly, partitioning will not occur unless the subduction interface at the base of the upper plate is considerably weaker than the material above it. Secondly, weak material within the overlying plate reduces the degree of partitioning of the velocity components. If these two features are combined in a subduction system, it is the strength of the base which controls the partitioning of the velocities. Weak material within the overlying plate can change the details but not the basic pattern of partitioning determined by basal strength.

[41] Thus, given a weak subduction interface, the surface signal landward of the trench that we would expect for oblique subduction is of approximately margin-parallel motion. Further from the trench the margin-normal component will be expressed and we would expect the surface measurement to reflect the subducting plate motion vector. The presence of a significant region of ponded sediment above the subduction interface would be manifest as a smaller degree of partitioning than predicted from the strength of the subduction interface. For a strong subduction interface, the two velocity components remain coupled, and we would expect to see the surface deformation close to the trench to reflect the plate motion vector. Further from the trench the motion should be a portion of the plate motion vector with the greatest gradient in both velocity components occurring at a significant distance from the trench.

5.3. Predicted Deformation Styles as a Function of Interfacial Strength

[42] We predict slightly oblique (dextral) normal faulting to occur in the northwest of the model, well away from the trench, where extensional deformation is taking place for the weak subduction interface. A weak subduction interface will also lead to thrust faulting at the trench, where the margin-normal velocity is decoupled from the margin-parallel velocity. Above the strong subduction zone all seismic activity should be away from the trench and will take the form of a mixture of oblique dextral and thrust events. Between the two regions a zone of dextral motion is predicted normal to the trench.

5.4. Comparison of Model Results With Northern New Zealand

[43] Extrapolation of kinematic data from northern New Zealand predicts clockwise rotation of the Hikurangi forearc with respect to the Australian plate, which is directly related to extension in the Taupo Volcanic Zone and its termination in the central North Island (Figure 7) [*Beanland and Haines, 1998*]. Constraints on this type of kinematic modeling include earthquake moment tensors, geodetic analysis, rates of deformation on major faults, and rates of vertical crustal motions. A major limitation of such a kinematic model is the lack of offshore data, an important consideration for northern New Zealand where the plate boundary is offshore (Figure 7). Thus this kinematic model is largely

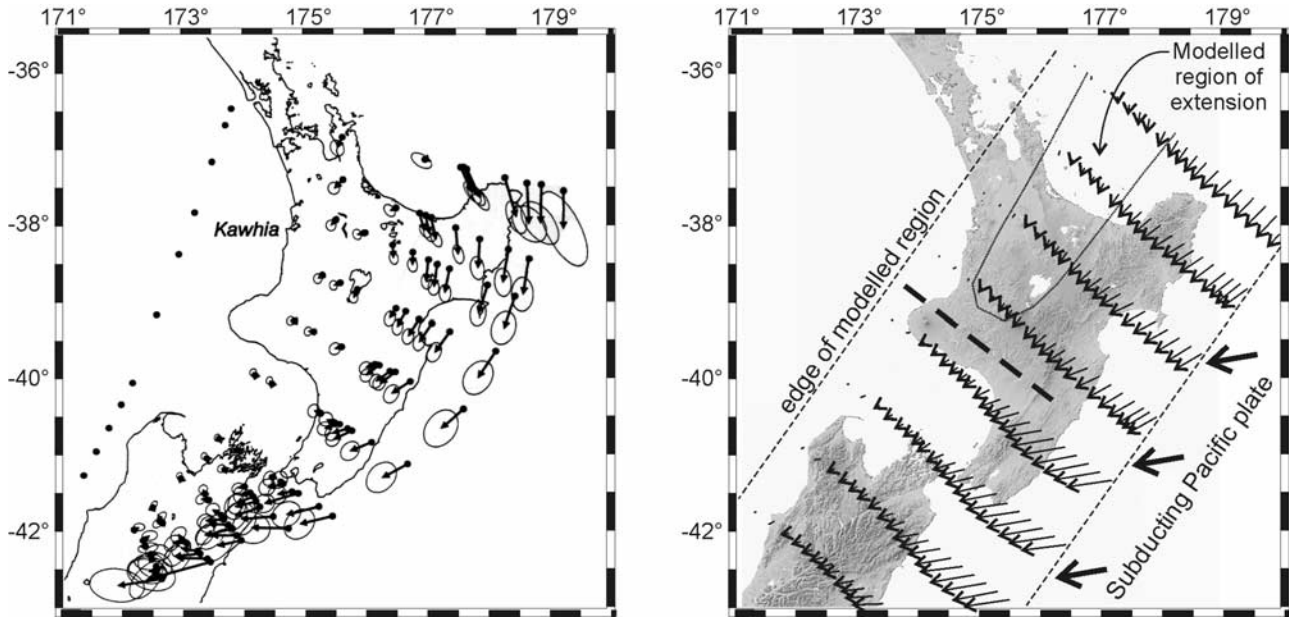


Figure 7. Comparison of the model with kinematic data modeling from northern New Zealand. (a) Basic solution from *Beanland and Haines* [1998] showing clockwise motion of the Hikurangi forearc with respect to the Australian plate (reprinted with permission from the Royal Society of New Zealand). (b) Surface velocity vectors from the model of oblique convergence with a weak subduction interface in the north and a strong interface in the south. The heavy dashed line denotes the boundary between the two regions. Boundary conditions are shown as bold arrows on the subducting Pacific plate and model results as light arrows on the Australian plate. The region of extension developed in the north is outlined.

unconstrained about the Hikurangi margin. Instead, strain and strain rates measurements in the Marlborough region appear to “pin” the model. Our dynamic models suggest that extension, along with strong partitioning of the margin-parallel and margin-normal components of velocity, will occur for a weakly coupled subduction interface but not where the interface is strongly coupled. This implies that it is the change in the strength of the subduction interface, strengthening to the south, that causes the reduction in the extension rate from north to south. Where a strong subduction interface exists, we predict very little partitioning between the two velocity components in agreement with the geodetic measurements for the southwest of the Hikurangi margin, where it is believed that there is strong coupling between the subducting plate and the overriding Australian plate.

[44] Between the two regions a zone of dextral motion is predicted normal to the trench, similar to that predicted by *Reyners* [1998] analysis of coupling changes along the Hikurangi margin. This zone extends from the trench, landward to about where the oblique thrust events in the south begin. The transition from a weak to a strong subduction interface occurs over a very small distance along strike in our models. In the North Island, the transition from weak to strong is gradual and occurs over a much greater distance [Reyners, 1998]. Thus we would expect that the region of margin-normal dextral motion developed as a result of the change from weak to strong subduction

interface would be diffuse and spread over most of the North Island.

5.5. Amount of Extension

[45] Present day rates of extension in the central Taupo Volcanic Zone range from Quaternary-averaged values of 6 mm yr^{-1} [Villamor and Berryman, 2001] to geodetic rates of $9 \pm 3 \text{ mm yr}^{-1}$ [Darby et al., 2000]. *Darby and Meertens* [1995] determined a value of $8 \pm 4 \text{ mm yr}^{-1}$ for the entire Taupo Volcanic Zone. These extension rates are $\sim 10\text{--}20\%$ of relative plate motion between the Australian and Pacific plates [DeMets et al., 1994]. Total extension in our models was $\sim 5\%$ of the imposed relative plate motion, implying that for the Taupo Volcanic Zone, one third to one half of the current extension rate can be accounted for by the geometry of the subduction zone and a weak subduction interface. The coexistence of processes such as slab rollback with this system would increase the amount of extension that takes place.

5.6. Weaker Material Beneath the Raukumara Peninsula

[46] Our models suggest that a block of weaker material within the upper plate will concentrate deformation at that point. Both margin-parallel and margin-normal strain is greatest above the region of weaker material, as is the vertical strain. A region of uplift develops above the region of weaker

material, with corresponding uplift rates of 4 mm yr^{-1} . This value, determined from the model, is comparable with measured uplift rates of 3 mm yr^{-1} [Yoshikawa *et al.*, 1980; Thornley, 1996] and supports Walcott's [1987] suggestion that sediment subduction and underplating are responsible for the uplift of the Raukumara Ranges.

6. Conclusions

[47] The strength of the subduction interface is a fundamental parameter in the determination of the mechanical behavior of a subduction zone and particularly that of the upper plate. Regions of weakness within the upper plate are reflected in the localization of deformation within the upper plate.

[48] Using the geometry of the Hikurangi margin of New Zealand, our models show that a weak subduction interface is required for both extension and partitioning of velocity

components to occur in a subduction zone of similar geometry. If the interface is stronger than the material of the overlying plate, neither extension nor partitioning of velocity components occurs.

[49] A weak region within the upper plate localizes all the components of displacement into that region, reducing the partitioning of velocity components above a weak subduction interface. A region of uplift, comparable to that observed in the Raukumara Ranges, develops above the region of weaker material.

[50] **Acknowledgments.** We thank Julie Rowland and Hugh Bibby for sharing their knowledge and insights into the geology of the Taupo Volcanic Zone. Thorough reviews from Dale Sawyer, David Evans, and an anonymous reviewer improved the clarity of the manuscript. This research was supported financially by the Univ. of Otago, and the Foundation of Research, Science and Technology (Contract UO0818). GeographX is acknowledged for the shaded relief map used in Figure 1.

References

- Anderson, H., and T. Webb, New Zealand seismicity: Patterns revealed by the upgraded National Seismograph Network, *N. Z. J. Geol. Geophys.*, **37**, 477–493, 1994.
- Anderson, H., E. Smith, and R. Robinson, Normal faulting in a back arc basin: Seismological characteristics of the March 2, 1987, Edgecumbe, New Zealand, earthquake, *J. Geophys. Res.*, **95**, 4709–4723, 1990.
- Ansell, J. H., and S. Bannister, Shallow morphology of the subducted Pacific plate along the Hikurangi margin, New Zealand, *Phys. Earth Planet. Inter.*, **93**, 3–20, 1996.
- Barnes, P. M., B. M. D. Lepinay, J.-Y. Collot, J. Delteil, and J.-C. Audru, Strain partitioning in the transition area between oblique subduction and continental collision, Hikurangi margin, New Zealand, *Tectonics*, **17**, 534–557, 1998.
- Beanland, S., The North Island dextral fault belt, Hikurangi subduction margin, New Zealand, Ph.D. thesis, Victoria Univ. of Wellington, Wellington, New Zealand, 1995.
- Beanland, S., and J. Haines, The kinematics of active deformation in the North Island, New Zealand, determined from geological strain rates, *N. Z. J. Geol. Geophys.*, **41**, 311–323, 1998.
- Beanland, S., A. Melhuish, A. Nicol, and J. Ravens, Structure and deformation history of the inner forearc region, Hikurangi subduction margin, New Zealand, *N. Z. J. Geol. Geophys.*, **41**, 325–342, 1998.
- Beck, M. E. J., On the mechanism of tectonic transport in zones of oblique subduction, *Tectonophysics*, **93**, 1–11, 1983.
- Chemenda, A., S. Lallemand, and A. Bokun, Strain partitioning and interplate friction in oblique subduction zones: Constraints provided by experimental modeling, *J. Geophys. Res.*, **105**, 5567–5581, 2000.
- Cundall, P., and M. Board, A microcomputer program for modeling of large-strain plasticity problems, in *Numerical Methods in Geomechanics: Proceedings of the 6th International Conference on Numerical Methods in Geomechanics*, vol. 2, edited by C. Swododa, pp. 101–108, Balkemapp, Innsbruck, Austria, 1988.
- Darby, D. J., and C. M. Meertens, Terrestrial and GPS measurements of deformation across the Taupo back arc and Hikurangi forearc regions in New Zealand, *J. Geophys. Res.*, **10**, 8221–8232, 1995.
- Darby, D. J., K. M. Hodgkinson, and G. H. Blick, Geodetic measurement of deformation in the Taupo Volcanic Zone, New Zealand: The north Taupo network revisited, *N. Z. J. Geol. Geophys.*, **43**, 157–170, 2000.
- DeMets, C., R. G. Gordon, D. F. Argus, and S. Stein, Effect of recent revisions to the geomagnetic reversal time scale on estimates of current plate motions, *Geophys. Res. Lett.*, **21**, 2191–2194, 1994.
- Dewey, J. F., Episodicity, sequence and style at convergent plate boundaries, in *The Continental Crust and Its Mineral Resources, Special Report 20*, edited by D. Strangeway, pp. 553–574, Geol. Assoc. of Can., Toronto, Ont., Canada, 1980.
- Eberhart-Phillips, D., and P. Chadwick, Three-dimensional attenuation model of the shallow Hikurangi subduction zone in Raukumara Peninsula, New Zealand, *J. Geophys. Res.*, **107**(B2), 2033, doi:10.1029/2000JB000046, 2002.
- Eberhart-Phillips, D., and M. Reyners, Plate interface properties in the northeast Hikurangi subduction zone, New Zealand, from converted seismic waves, *Geophys. Res. Lett.*, **26**, 2565–2568, 1999.
- Finch, T. J., Plate convergence, transcurrent faulting, and internal deformation adjacent to Southeast Asia and the western Pacific, *J. Geophys. Res.*, **77**, 4432–4460, 1972.
- Grindley, G. W., Sheet 8, Taupo, in *Geological Map of New Zealand*, N. Z. Dep. of Sci. and Ind. Res., Wellington, New Zealand, 1960.
- Hamilton, W. B., Subduction systems and magmatism, in *Volcanism Associated With Extension at Consuming Plate Margins*, edited by J. L. Smellie, *Geol. Soc. Spec. Publ.*, **81**, 3–28, 1995.
- Hassani, R., D. Jongmans, and J. Chery, Study of plate deformation and stress in subduction processes using two-dimensional numerical models, *J. Geophys. Res.*, **102**, 17,951–17,965, 1997.
- Hobbs, B. E., H.-B. Muhlhaus, and A. Ord, Instability, softening and localization of deformation, in *Deformation Mechanisms, Rheology and Tectonics*, edited by R. J. Knipe and E. H. Rutter, *Geophys. Res. Lett.*, **54**, 143–165, 1990.
- ITASCA, FLAC^{3D} (Fast Lagrangian Analysis of Continua in 3 Dimensions), Itasca Consulting Group Inc., Minneapolis, Minn., USA, 1997.
- Jarrard, R. D., Terrain motion by strike-slip faulting of fore arc slivers, *Geology*, **14**, 780–783, 1986.
- Liu, X., K. C. McNally, and Z. K. Shen, Evidence for a role of the downgoing slab in earthquake slip partitioning at oblique subduction zones, *J. Geophys. Res.*, **100**, 15,351–15,372, 1995.
- Mandl, G., *Mechanics of Tectonic Faulting*, Elsevier Sci., New York, 1988.
- McCaffrey, R., Oblique plate convergence, slip vectors, and forearc deformation, *J. Geophys. Res.*, **97**, 8905–8915, 1992.
- Molnar, P., and T. Atwater, Inter-arc spreading and cordilleran tectonics as alternatives related to the age of subducted oceanic lithosphere, *Earth Planet. Sci. Lett.*, **54**, 261–271, 1978.
- Ord, A., and N. H. S. Oliver, Mechanical controls on fluid flow during regional metamorphism: Some numerical models, *J. Metamorph. Geol.*, **15**, 345–359, 1997.
- Pacheco, J. F., L. R. Sykes, and C. H. Scholz, Nature of seismic coupling along simple plate boundaries of the subduction type, *J. Geophys. Res.*, **98**, 14,133–14,159, 1993.
- Reyners, M., Plate coupling and the hazard of large subduction thrust earthquakes at the Hikurangi subduction zone, New Zealand, *N. Z. J. Geol. Geophys.*, **41**, 343–354, 1998.
- Reyners, M., D. Eberhart-Phillips, and G. Stuart, A three-dimensional image of shallow subduction: Crustal structure of the Raukumara Peninsula, New Zealand, *Geophys. J. Int.*, **137**, 873–890, 1999.
- Rowland, J. V., and R. H. Sibson, Extensional fault kinematics within the Taupo Volcanic Zone, New Zealand: Soft-linked segmentation of a continental rift system, *N. Z. J. Geol. Geophys.*, **44**, 271–283, 2001.
- Ruff, L. J., Do trench sediments affect great earthquake occurrence in subduction zones, in *Subduction Zones: Part II*, edited by L. J. Ruff and H. Kanamori, pp. 268–282, Birkhauser Verlag, Basel, Switzerland, 1989.
- Scholz, C. H., and J. Campos, On the mechanism of seismic decoupling and back arc spreading at subduction zones, *J. Geophys. Res.*, **100**, 22,103–22,115, 1995.
- Taylor, B., and G. D. Karner, On the evolution of marginal basins, *Rev. Geophys.*, **21**, 1727–1741, 1983.
- Thornley, S., Neogene tectonics of Raukumara Peninsula, northern Hikurangi margin, New Zealand, Ph.D. thesis, Victoria Univ., Wellington, New Zealand, 1996.
- Uyeda, S., An introduction to comparative subductology, *Tectonophysics*, **81**, 133–159, 1982.

- Uyeda, S., and H. Kanamori, Back arc opening and the mode of subduction, *J. Geophys. Res.*, *84*, 1049–1059, 1979.
- Vermeer, P. A., and R. de Borst, Non-associated plasticity for soils, concrete and rock, *Heron*, *29*, 1–64, 1984.
- Villamor, P., and K. Berryman, A late Quaternary extension rate in the Taupo Volcanic Zone, New Zealand, derived from fault slip data, *N. Z. J. Geol. Geophys.*, *44*, 243–269, 2001.
- Walcott, R. L., The kinematics of the plate boundary zone through New Zealand: A comparison of short- and long-term deformation, *Geophys. J. R. Astron. Soc.*, *79*, 613–633, 1984.
- Walcott, R. L., Geodetic strain and deformational history of the North Island of New Zealand during the Cainozoic, *Philos. Trans. R. Soc. London, Ser. A*, *321*, 163–181, 1987.
- Webb, T. H., and H. Anderson, Focal mechanisms of large earthquakes in the North Island of New Zealand: Slip partitioning at an oblique active margin, *Geophys. J. Int.*, *134*, 40–86, 1998.
- Whittaker, A., M. H. P. Bott, and G. D. Waghorn, Stresses and plate boundary forces associated with subduction plate margins, *J. Geophys. Res.*, *97*, 11,933–11,944, 1992.
- Yoshikawa, T., Y. Ota, N. Yonekura, A. Okada, and N. Iso, Marine terraces and their tectonic deformation on the north-east coast of the North Island, New Zealand, *Geogr. Rev. Jpn.*, *53-4*, 238–262, 1980.
- Yu, G., S. G. Wesnousky, and G. Ekstrom, Slip partitioning along major convergent plate boundaries, *Pure Appl. Geophys.*, *140*, 183–210, 1993.
-
- D. Eberhart-Phillips, Institute of Geological and Nuclear Sciences, Private Bag 1930, Dunedin, New Zealand.
- P. O. Koons and P. Upton, Department of Earth Sciences, University of Maine, 5790 Bryand Global Sciences Center, Orono, ME 04469-5790, USA. (phaedra.upton@maine.edu)